environmental microbiology

Environmental Microbiology (2021) **23**(9), 5525–5540 doi:10.1111/1462-2920.15700

The bacterium *Pseudomonas protegens* antagonizes the microalga *Chlamydomonas reinhardtii* using a blend of toxins

Magdalena M. Rose,[1,2†] **Daniel Scheer**,[2†] **Yu Hou**,[2] **Vivien S. Hotter**,[2] **Anna J. Komor**,[3] **Prasad Aiyar**,[2] **Kirstin Scherlach**,[3] **Fredd Vergara**,[4,5] **Qing Yan**,[6] **Joyce E. Loper**,[7] **Torsten Jakob**,[1] **Nicole M. van Dam**,[4,5] **Christian Hertweck**,[3,8] **Maria Mittag**[2] and **Severin Sasso**[1,2,4*]

[1]*Institute of Biology, Leipzig University, Leipzig, Germany.*

[2]*Matthias Schleiden Institute of Genetics, Bioinformatics and Molecular Botany, Friedrich Schiller University Jena, Jena, Germany.*

[3]*Department of Biomolecular Chemistry, Leibniz Institute for Natural Product Research and Infection Biology (HKI), Jena, Germany.*

[4]*German Centre for Integrative Biodiversity Research (iDiv) Halle-Jena-Leipzig, Leipzig, Germany.*

[5]*Institute of Biodiversity, Friedrich Schiller University Jena, Jena, Germany.*

[6]*Department of Plant Sciences and Plant Pathology, Montana State University, Bozeman, Montana.*

[7]*Department of Botany and Plant Pathology, Oregon State University, Corvallis, Oregon.*

[8]*Faculty of Biological Sciences, Friedrich Schiller University Jena, Jena, Germany.*

Summary

The unicellular alga *Chlamydomonas reinhardtii* and the bacterium *Pseudomonas protegens* serve as a model to study the interactions between photosynthetic and heterotrophic microorganisms. *P. protegens* secretes the cyclic lipopeptide orfamide A that interferes with cytosolic Ca^{2+} homeostasis in *C. reinhardtii* resulting in deflagellation of the algal cells. Here, we studied the roles of additional secondary metabolites secreted by *P. protegens* using individual compounds and co-cultivation of algae with bacterial mutants. Rhizoxin S2, pyrrolnitrin, pyoluteorin, 2,4-diacetylphloroglucinol (DAPG) and orfamide A all induce changes in cell morphology and inhibit the growth of *C. reinhardtii*. Rhizoxin S2 exerts the strongest growth inhibition, and its action depends on the spatial structure of the environment (agar versus liquid culture). Algal motility is unaffected by rhizoxin S2 and is most potently inhibited by orfamide A (IC_{50} = 4.1 μM). Pyrrolnitrin and pyoluteorin both interfere with algal cytosolic Ca^{2+} homeostasis and motility whereas high concentrations of DAPG immobilize *C. reinhardtii* without deflagellation or disturbance of Ca^{2+} homeostasis. Co-cultivation with a regulatory mutant of bacterial secondary metabolism (Δ*gacA*) promotes algal growth under spatially structured conditions. Our results reveal how a single soil bacterium uses an arsenal of secreted antialgal compounds with complementary and partially overlapping activities.

Introduction

Eukaryotic microalgae and cyanobacteria fix large amounts of atmospheric CO_2 into organic carbon. These photosynthetic microorganisms are the dominant primary producers in aquatic ecosystems and contribute substantially to primary production in terrestrial ecosystems (Behrenfeld *et al*., 2001; Elbert *et al*., 2012). They can improve soils in various ways, for example, by promoting the formation and stability of soil aggregates (Metting, 1986; Alvarez *et al*., 2021). Microalgae and cyanobacteria serve as a food source for consumers at higher trophic levels of the food web (Schmidt *et al*., 2016). Their interactions with other microorganisms shape food webs and affect the course of biogeochemical cycles. Generally, the outcome of microbial encounters is determined by a chemical language consisting of nutrients, signals, and toxins (Schmidt *et al*., 2019). Microalgae engage in different types of microbial interactions that range from mutualistic to commensalistic and

Received 31 March, 2021; revised 24 June, 2021; accepted 31 July, 2021. *For correspondence. E-mail severin.sasso@uni-leipzig.de; Tel. (+49) 341 9736893; Fax (+49) 341 9736899. †These authors contributed equally to this work.

antagonistic (Hom *et al*., 2015; Ramanan *et al*., 2016). One type of antagonistic interaction involves algicidal bacteria that can kill microalgae through physical contact or by the release of detrimental metabolites or proteins (Mayali and Azam, 2004; Meyer *et al*., 2017). Algicidal bacteria may accelerate algal turnover rates and influence the dynamics of harmful algal blooms in the oceans (Meyer *et al*., 2017). Less is known about algicidal interactions in terrestrial habitats where the diffusion of secreted algicides appears more limited than in the open water.

The bacterium *Pseudomonas protegens* and the microalga *Chlamydomonas reinhardtii* are both found in soils. Together, they form an experimental model to mechanistically decipher antagonistic algal-bacterial interactions on the molecular level (Aiyar *et al*., 2017). *C*. *reinhardtii* is a unicellular alga found in nutrient-rich temperate soils and a model species for the study of fundamental biological processes and for ecotoxicological analyses (Nestler *et al*., 2012; Sasso *et al*., 2018). *P*. *protegens* strain Pf-5, formerly classified as *Pseudomonas fluorescens* (Ramette *et al*., 2011), is found in the rhizosphere and produces secondary metabolites including siderophores that protect land plants against microbial pathogens (Haas and Défago, 2005; Paulsen *et al*., 2005). For example, pyrrolnitrin possesses strong antifungal activity, while pyoluteorin is toxic to oomycetes and some fungi and bacteria (Gross and Loper, 2009). In *P*. *protegens*, the production of many secondary metabolites is regulated by a two-component system consisting of the sensor kinase GacS and the response regulator GacA (Kidarsa *et al*., 2013; Yan *et al*., 2018). A Δ*gacA* mutant is devoid of inhibitory activity against the fungal phytopathogen *Fusarium verticillioides* (Quecine *et al*., 2016).

C. *reinhardtii* and *P*. *protegens* constitute a genetically tractable dyad to investigate the role of secondary metabolites in algal-bacterial interactions. Aiyar *et al*. (2017) found that co-cultivation of *P*. *protegens* with *C*. *reinhardtii* results in growth inhibition, altered morphology and immobilization of the algae. They proposed that *P*. *protegens* produces toxins to obtain nutrients such as trace metals from *C*. *reinhardtii*. Orfamide A, a cyclic lipopeptide secreted by the bacteria, perturbs the homeostasis of calcium ions (Ca^{2+}) in the algal cytosol and causes deflagellation of *C*. *reinhardtii* (Aiyar *et al*., 2017). Spatial and temporal variations of cytosolic Ca^{2+} levels represent distinct signals that regulate many important processes such as flagellar function, light perception, or photosynthesis (Wheeler *et al*., 2008; Hochmal *et al*., 2016). However, experiments with an orfamide-deficient mutant (Δ*ofaA*) suggested that deflagellation and growth inhibition are not only caused by orfamide A but may involve other metabolites secreted by *P*. *protegens* (Aiyar *et al*., 2017).

In this work, we explored the role of additional secreted metabolites of *P*. *protegens* in its interaction with *C*. *reinhardtii* using purified compounds and co-cultivation experiments with mutants of *P*. *protegens* that lack different metabolites. The aim of our study is to further characterize the activities of bacterial metabolites on growth, morphology, Ca^{2+} homeostasis, deflagellation and motility of *C*. *reinhardtii*.

Results

C. reinhardtii *is affected by a mixture of secondary metabolites secreted by* P. protegens

P. *protegens* secretes various secondary metabolites (Gross and Loper, 2009) that may play important roles in the antagonistic interaction between *C*. *reinhardtii* and *P*. *protegens*. Secreted secondary metabolites were extracted using ethyl acetate from spent medium of *P*. *protegens* cultivated in Tris-Acetate-Phosphate medium (TAP). The extract inhibited the growth of *C*. *reinhardtii* on agar plates similar to the inhibition observed by co-culturing with bacterial cells (Fig. 1A). Liquid algal cultures exposed to the bacterial extracts for 24 h were likewise inhibited (Fig. 1B).

We used a previously established aequorin reporter strain of *C*. *reinhardtii* (Aiyar *et al*., 2017) to monitor possible perturbations in cytosolic Ca^{2+} homeostasis by the mixture of extracted secondary metabolites secreted by *P*. *protegens*. The extract induced a sharp spike in cytosolic Ca^{2+} in *C*. *reinhardtii* that peaked within less than a minute, followed by a weaker but continued Ca^{2+} elevation (Fig. 1C, Fig. S2A). Within 1 min, the algal cells also shed their flagella (also known as cilia) (Fig. 1D, left panel). Prolonged exposure to the extract for one day resulted in more severe morphological changes: algal cells lost their green colour, became slightly distended and failed to regrow their flagella (Fig. 1D, right panel, Fig. S1). Algal bleaching, cell distention and loss of flagella were also observed during co-culturing with *P*. *protegens* (Aiyar *et al*., 2017). These results show that one or more of the substances secreted by *P*. *protegens* contribute substantially to the adverse effects on *C*. *reinhardtii*.

Quantification of secondary metabolites in the spent culture medium

We tested whether the presence of *C*. *reinhardtii* alters the composition of secreted metabolites in *P*. *protegens*. Analyses by high-performance liquid chromatography coupled to a photodiode array detector

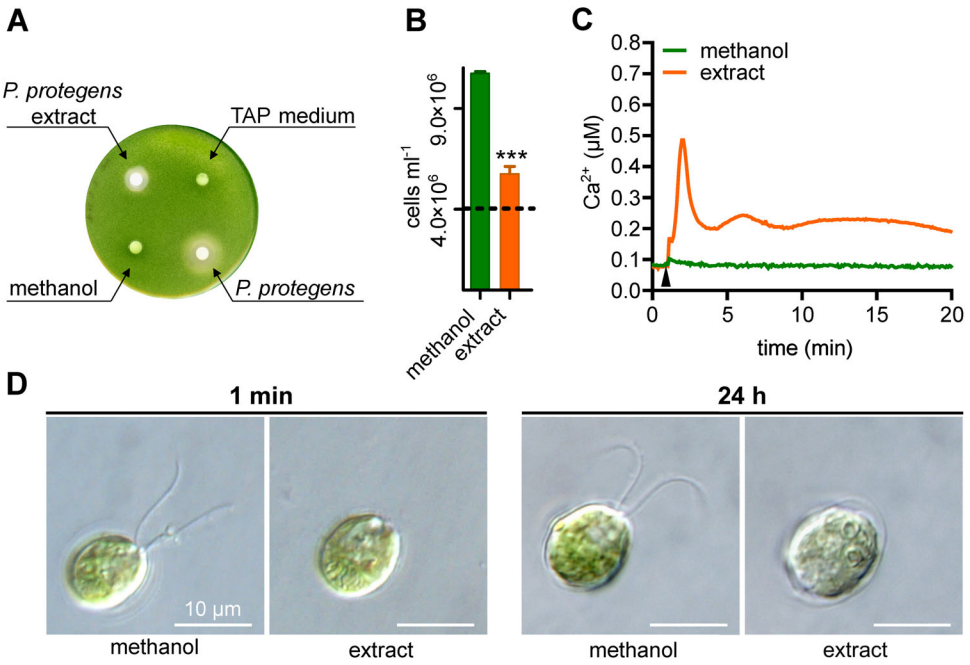

Fig. 1. The mixture of secondary metabolites secreted by *Pseudomonas protegens* negatively affects *Chlamydomonas reinhardtii*.
A. Inhibitory effect of live *P. protegens* and extracted secondary metabolites on algal growth on agar plates. Secreted secondary metabolites were extracted from the spent medium of a *P. protegens* culture. A volume of 10 μl extract dissolved in methanol was applied onto a filter disk on the surface of an agar plate inoculated with *C. reinhardtii*. These 10 μl of extract contained the compounds extracted from 3 ml of spent bacterial culture medium. As negative controls, 10 μl of TAP medium or methanol were used. This experiment was conducted twice with three biological replicates each.
B. Quantification of algal growth inhibition by secreted bacterial compounds. A volume of 10 μl extract of bacterial compounds was added to an algal cell suspension with an initial cell density of 4×10^6 cells ml^{-1} (dashed line), and algal growth was quantified after 24 h. For determining statistical significance, a student's *t*-test was performed (mean ± SD are shown, ***$p < 0.001$). This experiment was performed twice with three biological replicates.
C. Disruption of cytosolic Ca^{2+} levels in *C. reinhardtii* by extracted bacterial compounds. A black arrowhead indicates the addition of extract. A volume of methanol equivalent to the volume of extract was used as a negative control. Each line represents the mean of three biological replicates, and each biological replicate includes three technical replicates. The experiments were repeated twice independently, with the second experiment shown in Fig. S2A.
D. Morphological changes of *C. reinhardtii* cells after incubation with extracted bacterial secondary metabolites for 1 min or 24 h. As a negative control, a volume of methanol identical to the volume of extract was applied. Representative micrographs are shown (see Fig. S1 for more micrographs of cells after 24 h of incubation with the extract). This experiment was performed once with three biological replicates. Scale bar indicates 10 μm. In panels B, C and D, 1 ml of algal cell suspension treated with extract contained the compounds extracted from 3 ml of spent bacterial culture medium.

(HPLC-PDA) revealed that the chemical profiles of the spent growth medium of axenic *P. protegens* cultures and those of co-cultures with *C. reinhardtii* were very similar (Fig. 2). Consequently, we chose to conduct further experiments with the extract from axenic *P. protegens* cultures.

To identify specific compounds, the extract of secondary metabolites was spiked with suitable standards that were obtained commercially or purified from bacterial culture extracts (see Experimental Procedures). Using HPLC analysis, we identified pyoluteorin, 2,4-diacetylphloroglucinol (DAPG), pyrrolnitrin and rhizoxin S2 in the *P. protegens* culture extracts (Fig. 3A, Fig. S3A). Using liquid chromatography-mass spectrometry (LC–MS), we further detected orfamide A (Fig. S3B). The physiological concentrations of the compounds that had accumulated in the growth medium were quantified using standard curves (Fig. S4). After 2 days of cultivation, the metabolite concentrations ranged from 29 nM to 11 μM (Fig. 3B). At a concentration of 11 μM, orfamide A was clearly the most abundant compound (Fig. 3B). Rhizoxin S2, DAPG and pyrrolnitrin were detected at 200, 76 and 58 nM, respectively. Pyoluteorin showed the lowest abundance with a concentration of 29 nM.

2,4-Diacetylphloroglucinol, pyoluteorin, pyrrolnitrin, and orfamide A immobilize algal cells

We proceeded to test the inhibitory activity of individual compounds on algal growth under our cultivation conditions. Based on their inhibition zones on agar plates, all five bacterial compounds negatively affected the growth

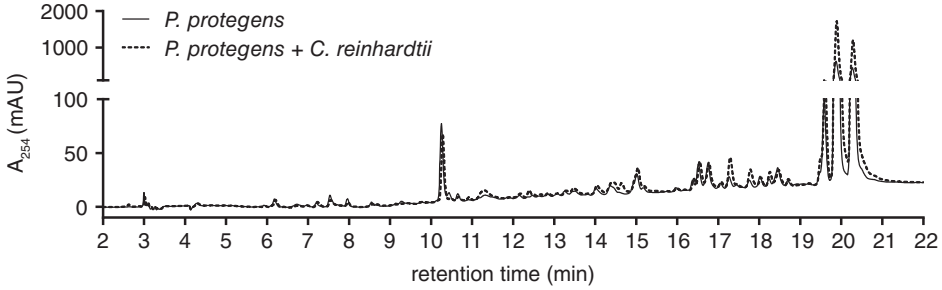

Fig. 2. The presence of *Chlamydomonas reinhardtii* does not alter the composition of secondary metabolites secreted by *Pseudomonas protegens*.
Overlay of HPLC-PDA chromatograms of secreted secondary metabolites extracted from spent medium of *P. protegens* in axenic culture (solid line) or in co-culture with *C. reinhardtii* (dashed line). The axenic culture of *P. protegens* was inoculated with a starting concentration of 1×10^7 cells ml^{-1}. The co-culture of *P. protegens* and *C. reinhardtii* was inoculated with the same bacterial starting concentration while algae were added at a concentration of 1×10^5 cells ml^{-1}, resulting in a ratio of 1:100 algae to bacteria. The cultures were incubated for 2 days prior to extraction. This experiment was performed twice independently with two biological replicates each.

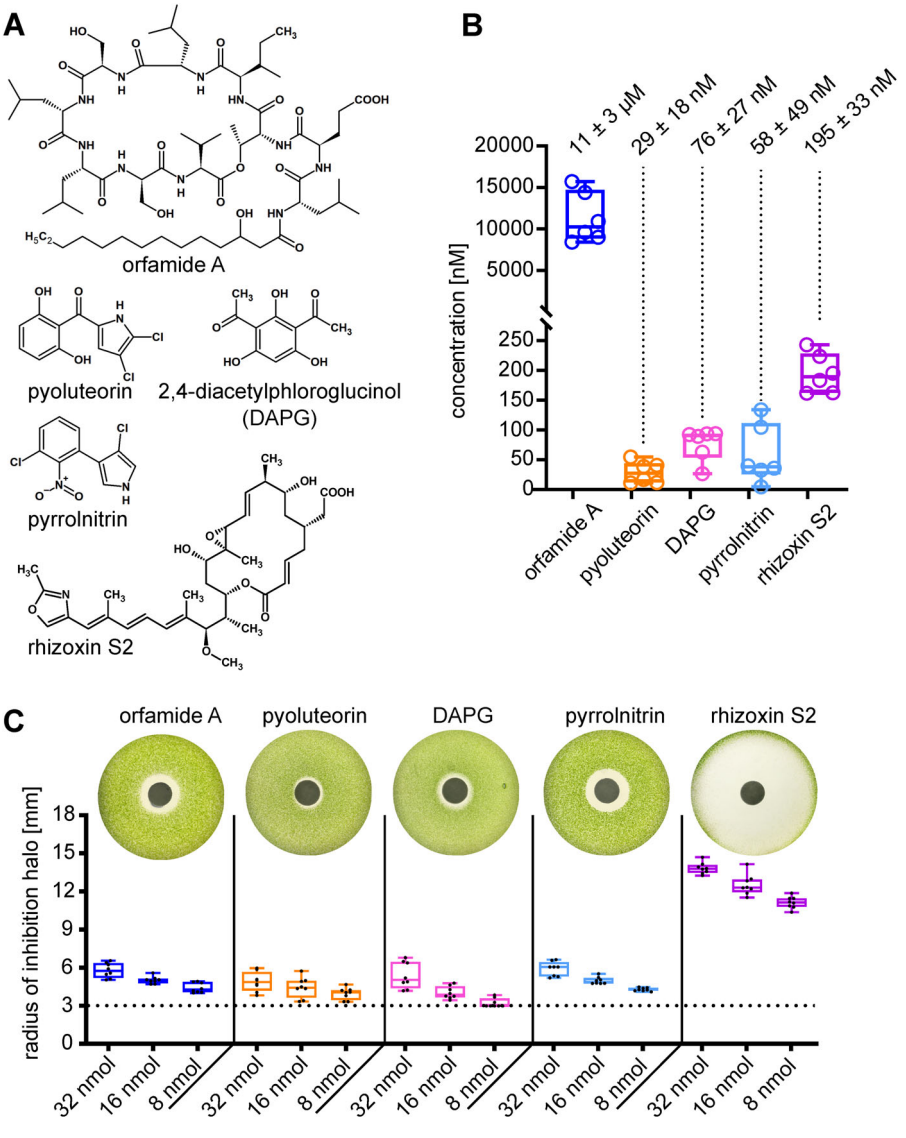

Fig. 3. Quantification of bacterial secondary metabolites and their effect on algal growth.
A. Chemical structures of secondary metabolites secreted by *P. protegens* in TAP medium. The structure of orfamide A is currently under revision (H.-D. Arndt, personal communication).
B. Physiological concentrations of orfamide A, pyoluteorin, 2,4-diacetyl phloroglucinol (DAPG), pyrrolnitrin and rhizoxin S2 accumulated in the TAP medium of 2-day old axenic *P. protegens* cultures grown under the same culture conditions as co-cultures. The compounds were identified and quantified via HPLC-PDA or in case of orfamide A by LC–MS (see Fig. S3, Fig. S4). The concentrations are expressed as mean ± SD (numbers above diagram) and data are depicted as box plots showing the median (horizontal line in the middle), interquartile range (boxes) and minimal and maximal values (whiskers). Each individual datapoint is shown as an empty circle.
C. Growth inhibition of *C. reinhardtii* by individual secondary metabolites on agar plates. Three different amounts of substance (32, 16 or 8 nmol) applied onto a 6 mm Ø filter disk were tested for orfamide A, pyoluteorin, DAPG, pyrrolnitrin and rhizoxin S2. Representative pictures of inhibition zones after treatment with 32 nmol are shown. The radii of the inhibition zones are depicted as box plots as in B. The dotted line indicates the radius of the filter disk. The depicted data consist of four plates with two technical replicates (filter disks) each, all of which are shown as individual data points.

of *C. reinhardtii*, with rhizoxin S2 exerting by far the strongest growth inhibition (Fig. 3C).

As orfamide A renders *C. reinhardtii* immotile through deflagellation within less than a minute (Aiyar *et al*., 2017), we tested whether pyoluteorin, DAPG, pyrrolnitrin or rhizoxin S2 immobilize the algal cells as well. To investigate this, algal-motility dose–response curves for each of these compounds were recorded. The half-maximal inhibitory concentration (IC_{50}) was calculated to facilitate comparison of the immobilizing potency amongst the tested compounds. We were able to determine IC_{50} values for four out of five compounds (Fig. 4A). The immobilizing activity ranged from $IC_{50} = 4.1$ μM (orfamide A, the most potent immobilizing compound) to $IC_{50} = 350$ μM (DAPG). Pyoluteorin and pyrrolnitrin had intermediary IC_{50} values of 95 μM and 20 μM, respectively (Fig. 4A). Despite its strong inhibition of algal growth on agar plates (Fig. 3C), rhizoxin S2 did not compromise the motility of *C. reinhardtii* even at a concentration as high as 160 μM (Fig. S5).

To investigate whether the loss of motility is correlated with deflagellation, we visually assessed whether cells

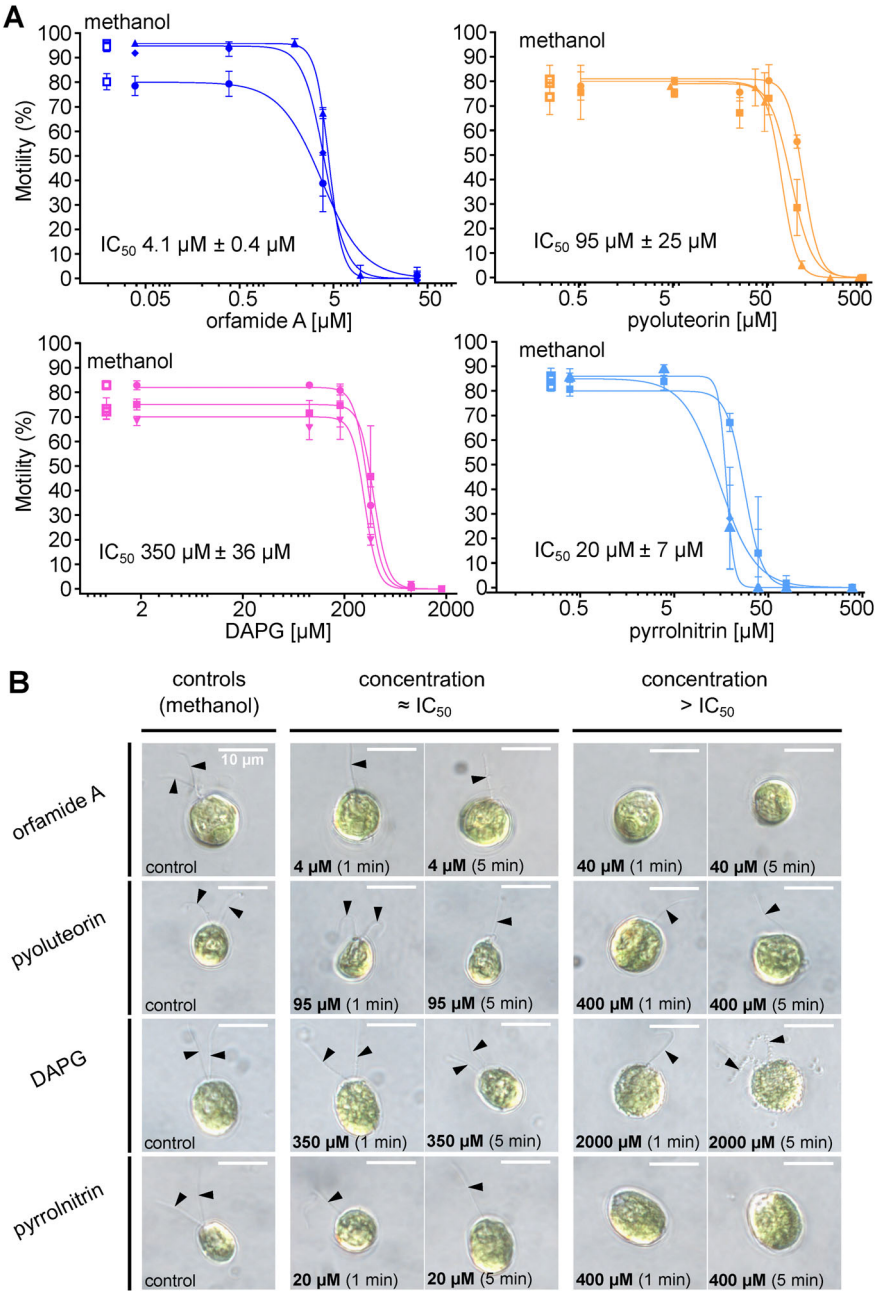

Fig. 4. Orfamide A, pyoluteorin, DAPG and pyrrolnitrin immobilize *Chlamydomonas reinhardtii* with or without deflagellation.
A. Influence of compounds secreted by *P. protegens* on the motility of *C. reinhardtii*. Dose–response curves were acquired to determine the half-maximal inhibitory concentration (IC_{50}), at which half of *C. reinhardtii* cells stop moving. IC_{50} values are expressed as mean ± SD (calculated from the three depicted curves). Empty squares indicate a treatment with methanol (negative control). Each data point represents the average of three technical replicates. Rhizoxin S2 did not affect algal motility up to a concentration of 160 μM (Fig. S5).
B. Flagellation status of *C. reinhardtii* after treatment with bacterial secondary metabolites. Representative differential interference contrast pictures are shown, which were taken after 1 or 5 min of treatment at the respective IC_{50} concentration and a concentration > IC_{50}. In case of orfamide A and pyrrolnitrin, many flagellated and completely deflagellated cells were found in addition to uniflagellated cells at the respective IC_{50} concentration. Methanol was added as a negative control. The presence of flagella is highlighted with black arrowheads. Scale bar = 10 μm. All treatments were conducted twice in three biological replicates each.

retained their flagella by microscopy. Like orfamide A, pyrrolnitrin was found to quickly deflagellate *C. reinhardtii* within minutes (Fig. 4B). In contrast, *C. reinhardtii* cells exposed to DAPG showed almost no deflagellation – even at a concentration nearly six times higher than its IC_{50}. Pyoluteorin treatment in the IC_{50}-concentration range predominantly resulted in uniflagellar *C. reinhardtii* (loss of one flagellum only). Even at pyoluteorin concentrations four times higher than the IC_{50} value, most cells were uniflagellated (Fig. 4B). Taken together, we found that only orfamide A and pyrrolnitrin appear to immobilize *C. reinhardtii* by complete deflagellation. In contrast, pyoluteorin predominantly led to a partial deflagellation, while DAPG immobilized algal cells without deflagellation.

Pyrrolnitrin and pyoluteorin induce cytosolic Ca^{2+} fluxes in C. reinhardtii *but do not disrupt the algal membrane*

Since deflagellation is tightly linked to calcium signalling (Wheeler *et al*., 2008), we examined whether the immobilizing effects of DAPG, pyoluteorin and pyrrolnitrin are caused by changes in the Ca^{2+} homeostasis in *C. reinhardtii*. For these experiments, we used concentrations corresponding to their half-maximal effect (IC_{50}) on motility determined earlier. A sharp and sudden rise of cytosolic Ca^{2+} in the algae was induced when they were exposed to 20 μM pyrrolnitrin (Fig. 5A, Fig. S2B). At a concentration of 100 μM, pyoluteorin treatment also led to a Ca^{2+} increase but the level rose more slowly compared to the signal obtained for pyrrolnitrin. DAPG, to the contrary, did not perturb the Ca^{2+} equilibrium at concentrations as high as 350 μM (Fig. 5A, Fig. S2B).

We further investigated whether the compounds of interest trigger the increase in Ca^{2+} by permeabilizing the algal cells. For this, we utilized Evans blue, a dye that enters membrane-compromised cells and is widely used to indicate cell death in *C. reinhardtii* (Crutchfield *et al*., 1999). Mastoparan, a known permeabilizing agent (Yordanova *et al*., 2013), was employed as a positive control. Exposure to 10 μM mastoparan for 30 s led to a staining of ~90% of algal cells (Fig. 5B). In contrast, neither pyoluteorin nor pyrrolnitrin permeabilized the cell membrane of *C. reinhardtii* cells at their respective IC_{50} concentrations (Fig. 5B). Like orfamide A (Aiyar *et al*., 2017), these bacterial metabolites thus may interfere with the algal Ca^{2+} homeostasis by a mechanism independent of membrane disruption.

Several compounds hamper the growth and change the morphology of C. reinhardtii

To investigate if the compounds secreted by *P. protegens* influence algal propagation, algal cell

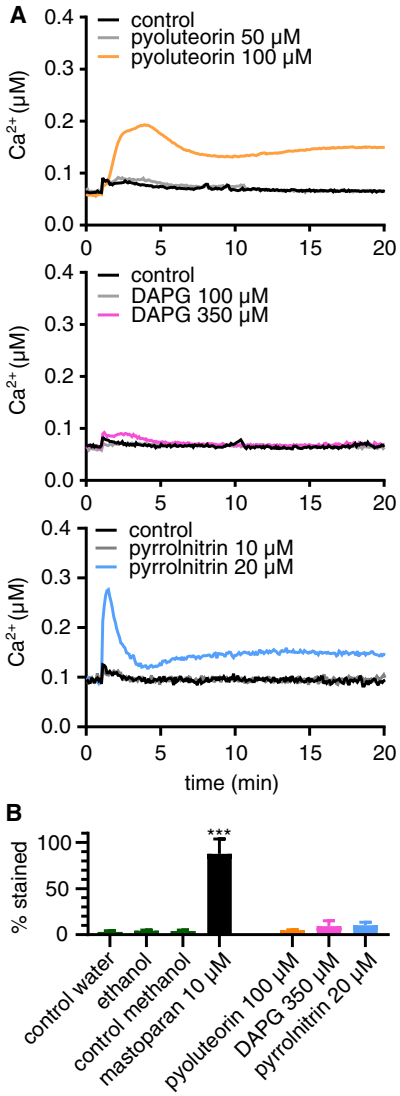

Fig. 5. Pyoluteorin and pyrrolnitrin influence the cytosolic calcium homeostasis of *Chlamydomonas reinhardtii*.
A. Effects of DAPG, pyoluteorin and pyrrolnitrin on cytosolic Ca^{2+} levels in *C. reinhardtii*. The highest concentrations chosen correspond to IC_{50} values of the metabolites' activity on motility (cf. Figure 4A). Black arrowheads indicate the addition of the metabolites. Ethanol or methanol equivalent to the volume of the tested compound (pyoluteorin dissolved in ethanol, DAPG and pyrrolnitrin dissolved in methanol) were used as negative controls. Each line represents the mean of three biological replicates, and each biological replicate includes three technical replicates. The experiments were repeated twice independently, with the second experiment shown in Fig. S2B.
B. Capability of the individual secondary metabolites to permeabilize the cell membrane of *C. reinhardtii*. Evans blue staining was used as an indicator for cell membrane permeabilization and viability. Mastoparan was used as a positive control; methanol was used as a negative control for DAPG and pyrrolnitrin, ethanol for pyoluteorin and water for mastoparan. This experiment was performed three times independently with three technical replicates each. At least 500 cells per technical replicate were evaluated. For the determination of statistically significant differences compared to the corresponding negative control, a one-way ANOVA followed by Tukey's multiple comparisons *post hoc* test was performed (mean ± SD are shown, ***$p < 0.001$).

suspensions were exposed to individual compounds for 24 h. At concentrations corresponding to their half-maximal effect on motility, pyrrolnitrin ($IC_{50} = 20$ μM) and DAPG (350 μM) completely inhibited the growth of *C. reinhardtii* (Fig. 6). The same effect was observed with 160 μM of rhizoxin S2. On the other hand, 4 μM orfamide A or 100 μM pyoluteorin significantly inhibited but did not abolish algal growth (Fig. 6).

To monitor further potential changes, algal cell morphology was visually assessed by taking micrographs after 24 h of exposure to the individual compounds. Morphological changes ranged from distended and deflagellated cells to more severely damaged cells that were bleached and granular. Algal cell morphologies were quite heterogenous for each treatment (Fig. S1). Orfamide A, DAPG, pyoluteorin, pyrrolnitrin and rhizoxin S2 all significantly or completely inhibited algal growth and caused a variety of morphological changes. Of these compounds, pyrrolnitrin induced the most extensive alterations in algal cell morphology after prolonged exposure.

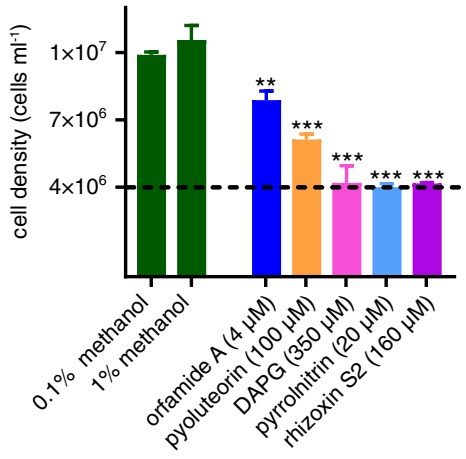

Fig. 6. DAPG, pyrrolnitrin and rhizoxin S2 prevent the growth of *Chlamydomonas reinhardtii* in liquid cultures.
Algal cell densities are shown after cultivation with or without individual bacterial secondary metabolites. The individual compounds were added to an algal cell suspension with an initial cell density of 4×10^6 cells ml^{-1} (dashed line), and algal growth was quantified after 24 h. The concentrations chosen correspond to IC_{50} values of the metabolites' activity on motility (cf. Figure 4A), except for rhizoxin S2, which was used at 160 μM. Methanol with the same volume as the compounds dissolved in methanol was added as a negative control (0.1% for orfamide A and pyrrolnitrin and 1% for pyoluteorin, DAPG and rhizoxin S2). For determining statistical significance, a one-way ANOVA followed by Tukey's multiple comparisons *post hoc* test was performed (mean ± SD are shown, $^{**}p < 0.01$, $^{***}p < 0.001$). This experiment was performed twice independently with three biological replicates each. All replicates are displayed.

P. protegens mutants reveal the importance of the different compounds in vivo

We further assessed the *in vivo* action of the secreted bacterial compounds by co-cultivating *C. reinhardtii* with mutants of *P. protegens* unable to produce one or several secondary metabolites (Table 1). Almost all tested single mutants inhibited the growth of *C. reinhardtii* on agar plates as strongly as wild-type *P. protegens* (Fig. 7A, Table S1). These mutants included Δ*phlA* (no DAPG and MAPG (monoacetylphloroglucinol)), Δ*phlD* (no DAPG, MAPG and pyoluteorin), Δ*pltA* (no pyoluteorin), Δ*prnC* (no pyrrolnitrin), Δ*hcnB* (no HCN) Δ*toxB* (no toxoflavin), and Δ*pvdL* (no pyoverdin). Only the Δ*rzxB* single mutant (no rhizoxins) showed a significantly smaller inhibition zone on agar plates than the wild type (Fig. 7A, left and middle panels, Table S1). A Δ*rzxB* mutation consistently reduced inhibitory activity in different biosynthetic mutants (Fig. 7A, Table S1). The Δ*gacA* mutant lacking the transcriptional activator GacA was unable to attenuate algal growth and even appeared to be growth promoting on agar plates (Fig. 7A right panel).

Contrary to the effect observed on agar plates, the Δ*gacA* mutant weakly inhibited the growth of *C. reinhardtii* in liquid cultures (Fig. 7B). The Δ*rzxB* mutant, which had diminished inhibitory activity on *C. reinhardtii* on agar plates, inhibited the algal growth in liquid cultures as strongly as the wild type. All other mutants with deletions in one to four biosynthesis genes inhibited algal growth in liquid co-cultures to a similar extent as the wild type (Fig. 7B, Fig. S6). By comparison, *C. reinhardtii* grew better in co-culture with *P. protegens* mutants with deletions in five, six, or seven antibiotic biosynthesis genes (Fig. 7B). However, these 5+ deletion mutants still altered the cell morphology of *C. reinhardtii* within 24 h in liquid cultures. Only algae co-cultured with the Δ*gacA* mutant appeared morphologically normal (Fig. 7C, Fig. S7). In summary, these results support a major role of GacA-regulated secondary metabolites in this antagonistic interaction, with the rhizoxins produced by *P. protegens* being elementary for algal growth inhibition in the spatially structured environment of agar plates.

Discussion

The soil bacterium *P. protegens* is toxic to a variety of organisms such as bacteria, fungi, oomycetes, or insects (Haas and Défago, 2005; Loper *et al*., 2016). Antibiotics produced by *P. protegens* include orfamide A, rhizoxins, hydrogen cyanide, pyrrolnitrin, pyoluteorin, toxoflavin and DAPG (Howell and Stipanovic, 1979, 1980; Nowak-Thompson *et al*., 1994; Gross *et al*., 2007; Loper *et al*., 2008; Loper

Table 1. List of *Pseudomonas protegens* strains and mutants used in this study.

Strains	Genotype	Description[a]	Reference
Pf-5	wild type (WT)		Paulsen *et al*., 2005
JL4577	Δ*gacA*	Altered in the many phenotypes regulated by GacA	Hassan *et al*., 2010
LK023	Δ*phlA*	DAPG$^-$, MAPG$^-$	Kidarsa *et al*., 2011
JL480	Δ*phlD*	DAPG$^-$ MAPG$^-$, Plt$^-$	Brazelton *et al*., 2008; Kidarsa *et al*., 2011
JL4805	Δ*pltA*	Plt$^-$	Henkels *et al*., 2014
JL4793	Δ*prnC*	Prn$^-$	Henkels *et al*., 2014
JL4808	Δ*rzxB*	Rzx$^-$	Henkels *et al*., 2014
JL4809	Δ*hcnB*	HCN$^-$	Loper *et al*., 2012
JL4832	Δ*toxB*	Tox$^-$	Quecine *et al*., 2016
JL3975	Δ*pvdL*	Pvd$^-$	Hartney *et al*., 2011
JL4830	Δ*phlD* Δ*prnC*	DAPG$^-$, MAPG$^-$, Plt$^-$, Prn$^-$	Quecine *et al*., 2016
LK026	Δ*phlA* Δ*prnC*	DAPG$^-$, MAPG$^-$, Prn$^-$	Henkels *et al*., 2014
LK027	Δ*phlA* Δ*rzxB*	DAPG$^-$, MAPG$^-$, Rzx$^-$	Henkels *et al*., 2014
JL4901	Δ*phlD* Δ*rzxB*	DAPG$^-$, MAPG$^-$, Plt$^-$, Rzx$^-$	Quecine *et al*., 2016
JL4902	Δ*prnC* Δ*rzxB*	Prn$^-$, Rzx$^-$	Quecine *et al*., 2016
JL4836	Δ*toxB* Δ*rzxB*	Tox$^-$ Rzx$^-$	Quecine *et al*., 2016
JL4844	Δ*phlD* Δ*rzxB* Δ*prnC*	Prn$^-$, DAPG$^-$, MAPG$^-$, Plt$^-$, Rzx$^-$	Quecine *et al*., 2016
LK031	Δ*phlA* Δ*rzxB* Δ*prnC*	Prn$^-$, DAPG$^-$, MAPG$^-$, Rzx$^-$	Henkels *et al*., 2014
JL4855	Δ*phlD* Δ*rzxB* Δ*prnC* Δ*pltA*	Prn$^-$, DAPG$^-$, MAPG$^-$, Plt$^-$, Rzx$^-$	Quecine *et al*., 2016
JL4865	Δ*phlD* Δ*rzxB* Δ*prnC* Δ*hcnB* Δ*pltA* (5xKO)	Prn$^-$, DAPG$^-$, MAPG$^-$, Plt$^-$, Rzx$^-$, HCN$^-$	Quecine *et al*., 2016
JL4909	Δ*phlD* Δ*rzxB* Δ*prnC* Δ*hcnB* Δ*pltA* Δ*ofaA* (6XKO)	Prn$^-$, DAPG$^-$, MAPG$^-$, Plt$^-$, Rzx$^-$, HCN$^-$, Ofa$^-$	Quecine *et al*., 2016
JL4932	Δ*phlD* Δ*rzxB* Δ*prnC* Δ*hcnB* Δ*pltA* Δ*ofaA* Δ*toxB* (7XKO)	Prn$^-$, DAPG$^-$, MAPG$^-$, Plt$^-$, Rzx$^-$, HCN$^-$, Ofa$^-$, Tox$^-$	Quecine *et al*., 2016

[a]Abbreviations: DAPG, 2,4-diacetylphloroglucinol; MAPG, monoacetylphloroglucinol; Plt, pyoluteorin; Prn, pyrrolnitrin; Rzx, rhizoxin derivatives; HCN, hydrogen cyanide; Tox, toxoflavin; Pvd, pyoverdin; Ofa, orfamide A.

et al., 2016). For orfamides, an inhibitory effect on the growth of the unicellular alga *C. reinhardtii* was demonstrated (Aiyar *et al*., 2017). However, the identity and modes of action of additional metabolites in the biotic interaction with *C. reinhardtii* remained unknown. These aspects were addressed in the current study.

An extract of compounds secreted by *P. protegens* induced similar inhibitory effects (Fig. 1) as live cells (Aiyar *et al*., 2017) with respect to algal growth inhibition, deflagellation and changes in cytosolic Ca^{2+} concentrations. In these extracts, we identified orfamide A, pyoluteorin, DAPG, pyrrolnitrin and rhizoxin S2 and quantified their concentrations. Orfamide A was the most abundant compound with a much higher concentration (11 μM) than observed for the other identified metabolites (30–200 nM; Fig. 3B). The concentrations of these metabolites are one to three orders of magnitude lower than those reported for *P. protegens* in a previous study (Quecine *et al*., 2016). These differences may be explained by the different culture media and the differing extraction method used by Quecine *et al*. (2016).

To quantify antialgal activity and to provide insights into the modes of action of the specific bacterial compounds, algal cells were treated with the individual compounds. Each of the five compounds attenuated the growth of *C. reinhardtii* on agar plates in a dose-dependent manner (Fig. 3C, Table 2). Remarkably, rhizoxin S2 inhibited algal growth on agar plates much more strongly than other compounds tested. The role of rhizoxin was confirmed by the growth tests, where *C. reinhardtii* was co-cultured with *P. protegens* mutants. This showed that all mutants with a Δ*rzxB* mutation reduced growth on agar plates less than the corresponding strains without an Δ*rzxB* mutation (Fig. 7A). This effect was much less prominent in liquid medium (Fig. 7, Fig. S6), suggesting that rhizoxins have a more important role on agar plates compared to liquid cultures (see also below). *P. protegens* can produce at least seven rhizoxin derivatives including rhizoxin S2 and the corresponding variant WF-1360 F with a δ-lactone ring (Brendel *et al*., 2007; Loper *et al*., 2008), and it is possible that multiple rhizoxins co-eluted under our HPLC conditions. Rhizoxin S2 and WF-1360 F also inhibit the proliferation of human cells (Scherlach *et al*., 2006). The antimitotic activity of rhizoxins depends on its interaction with β-tubulin. A conserved asparagine residue (Asn-100) in β-tubulin is critical for rhizoxin binding, and its mutation confers resistance to rhizoxin (Takahashi *et al*., 1990; Prota *et al*., 2014). The Asn-100 present in β-tubulin of *C. reinhardtii* (Youngblom *et al*., 1984) is in agreement with its high sensitivity to rhizoxin S2. To our knowledge, this is the first evidence of an antagonistic effect of rhizoxin analogues on microalgae.

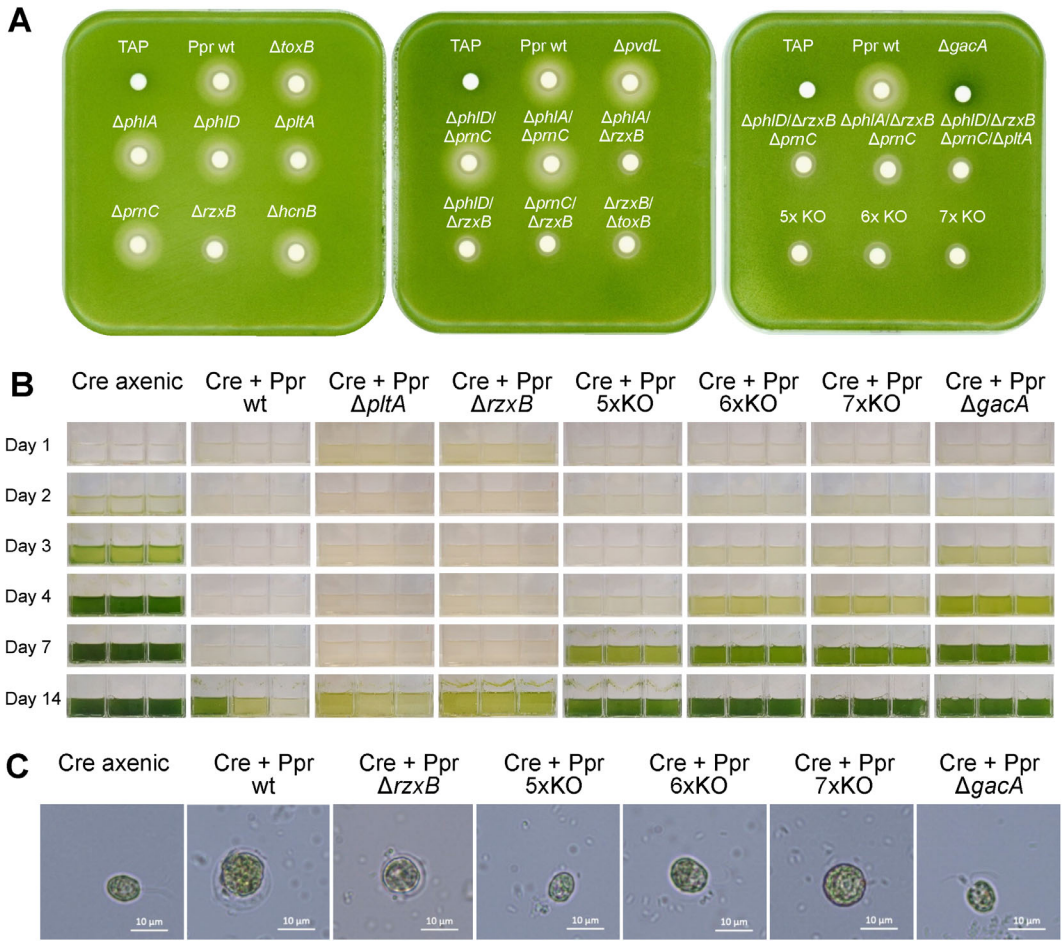

Fig. 7. *Pseudomonas protegens* mutants differentially affect the growth of *Chlamydomonas reinhardtii* on agar plates and in liquid medium.
A. Co-cultivation of *C. reinhardtii* with *P. protegens* mutants on agar plates. Filter disks were inoculated with 10 µl of *P. protegens* cell suspension adjusted to a concentration of 7×10^7 cells ml^{-1}. Information on the different mutants and abbreviations are provided in Table 1.
B. Co-cultivation of *C. reinhardtii* (Cre) with *P. protegens* (Ppr) mutants in liquid cultures. Cultures were inoculated with an initial cell density of 8.3×10^4 algae ml^{-1} and 8.3×10^6 bacteria ml^{-1} (starting ratio = 1:100). Additional results of co-cultures are shown in Fig. S6.
C. Morphological changes of algal cells after co-cultivation with *P. protegens* mutants for 24 h. Representative bright field micrographs are shown. Additional micrographs are depicted in Fig. S7.

Table 2. Summary of the activities of secreted metabolites from *Pseudomonas protegens* on *Chlamydomonas reinhardtii*.

Compound	Growth inhibition on plates[a]	Growth inhibition in liquid medium[a]	Morphology changes after 24 h	Induction of cell p ermeability	Deflagellation[a]	Calcium signal	Motility IC_{50}
Pyoluteorin	+	++	Yes	No	+	Yes	95 µM
DAPG	+	+++	Yes	No	−	No	350 µM
Orfamide A	+	++	Yes	No[b]	+++	Yes[b]	4.1 µM
Pyrrolnitrin	+	+++	Yes	No	+++	Yes	20 µM
Rhizoxin S2	+++	+++	Yes	n/a[c]	−	n/a	> 160 µM

[a]+ = weak, ++ = medium, +++ = strong, − = none.
[b]Data from Aiyar *et al*.
[c]n/a = not assessed.

A previous study demonstrated that orfamide A causes a rapid deflagellation and loss of motility (within less than a minute) in *C. reinhardtii* (Aiyar *et al*., 2017). Here, we examined if other bacterial metabolites can deflagellate and immobilize algal cells. In agreement with its mode of action discussed above, rhizoxin S2 neither induced immobilization nor deflagellation of *C. reinhardtii* up to a concentration of 160 µM (Fig. S5). In contrast, an

immobilizing effect on *C. reinhardtii* was evident for orfamide A, pyrrolnitrin, pyoluteorin and DAPG (Table 2). Notably, orfamide A was the most potent inhibitor of motility, and its IC_{50} value of 4 μM (Fig. 4A) matches the concentrations (≥2 μM) that disrupt Ca^{2+} homeostasis in *C. reinhardtii* (Aiyar *et al*., 2017). Moreover, the dose-dependent inhibition of motility by orfamide A coincided with its deflagellating activity (Fig. 4B). The mechanistic link between the orfamide-induced Ca^{2+} elevation and deflagellation is in agreement with the results of Aiyar *et al*. (2017) who provided evidence that orfamide A hampers the motility of *C. reinhardtii* not by membrane permeabilization but by direct targeting of Ca^{2+} channels.

Like orfamide A, pyrrolnitrin quickly induces cytosolic Ca^{2+} elevations and deflagellation at a concentration of 20 μM without impairing membrane integrity (Table 2). Therefore, pyrrolnitrin is probably one of the metabolites previously suspected (Aiyar *et al*., 2017) to deflagellate *C. reinhardtii* in addition to orfamide A. Furthermore, 20 μM pyrrolnitrin not only compromised the motility of *C. reinhardtii*, but also abolished its growth in liquid culture (Fig. 6). Pyrrolnitrin is known to inhibit the respiratory chain in *Saccharomyces cerevisiae*, with 50% inhibition at ∼20 μM pyrrolnitrin (Tripathi and Gottlieb, 1969). It is conceivable that the growth-inhibitory effect of pyrrolnitrin on *C. reinhardtii* relies on the same mechanism.

The effects of pyoluteorin and DAPG on motility, deflagellation, and Ca^{2+} signalling differ from the effects of pyrrolnitrin and orfamide A. While both pyoluteorin and DAPG inhibited algal motility, many algal cells retained flagella at immobilizing concentrations of these metabolites (Fig. 4). In case of pyoluteorin, uniflagellated cells were often observed (Fig. 4B). Uniflagellated cells were previously observed after shearing (Rosenbaum *et al*., 1969) while we showed that uniflagellated cells can be chemically induced as well. Despite the long-known antibiotic activity of pyoluteorin against the oomycete *Pythium ultimum* (Howell and Stipanovic, 1980), little is known about its mode of action. In human cancer cells, pyoluteorin induces cell cycle arrest, possibly via reduction of the mitochondrial membrane potential (Ding *et al*., 2020). It remains to be tested if a similar mechanism is responsible for the growth cessation observed in *C. reinhardtii* (Fig. 6). DAPG, on the other hand, barely affected Ca^{2+} homeostasis in *C. reinhardtii* at a motility-compromising concentration of 350 μM (Fig. 5A). This stands in contrast to the effect on *Neurospora crassa*, where ∼70 μM DAPG elicited a clear rise in cytosolic Ca^{2+} (Troppens *et al*., 2013b). Since DAPG did not deflagellate *C. reinhardtii* (Fig. 4B), the mechanism of immobilization by DAPG appears to differ fundamentally from orfamide A and pyrrolnitrin. DAPG is known for its broad antifungal, antibacterial, and phytotoxic activity (Weller *et al*., 2002). Based on experiments with *S. cerevisiae*, the primary mode of action of DAPG is the dissipation of the mitochondrial proton gradient, uncoupling electron transport and ATP synthesis and ultimately resulting in growth inhibition (Troppens *et al*., 2013a). DAPG also induces reactive oxygen species in *S. cerevisiae*, may inactivate vacuolar ATPase, and at higher concentrations increases membrane permeability (Kwak *et al*., 2011). Since 350 μM DAPG completely abolished the growth of *C. reinhardtii* (Fig. 6), it is conceivable that motility was not directly targeted by DAPG but instead was inhibited by limitation of mitochondrial respiration and supply of cellular energy.

Except for orfamide A, the individual secondary metabolites exerted physiological effects on *C. reinhardtii* only at much higher concentrations than those found in the spent medium of *P. protegens*. In contrast to experiments with the individual compounds, however, the situation in the algal-bacterial mixed cultures is more complex. For example, the concentrations of the secreted metabolites in the medium may change over time due to accumulation, degradation or uptake. Moreover, *P. protegens* was observed to actively swim towards *C. reinhardtii* (Aiyar *et al*., 2017), a behaviour potentially resulting in locally increased concentrations of secreted bacterial metabolites around algal cells. Finally, the characterized bacterial metabolites have overlapping activities and hence act in a cooperative fashion. Therefore, additional experiments were performed with *P. protegens* biosynthetic mutants in co-culture with *C. reinhardtii*. The results of the experiments in liquid cultures collectively support a cooperative action of antialgal compounds: (a) Mutations in at least five biosynthesis genes were necessary in *P. protegens* to improve algal growth compared to co-cultivation with wild-type *P. protegens* (Fig. 7B), (b) apart from Δ*gacA*, all mutants, including the mutant with deletions in seven biosynthesis genes, induced deflagellation and morphological changes in *C. reinhardtii* (Fig. 7C, Fig. S7).

The co-cultivation of *C. reinhardtii* with the Δ*rzxB* and Δ*gacA* mutants of *P. protegens* showed some pronounced differences between agar plate assays and liquid cultures (Fig. 7). Various factors may account for these differences such as diffusion, mixing, physical contact and physiological state of the cells. The spatial structure of the environment can strongly influence the action of antibiotics in microbial communities (Wiener, 2001; Westhoff *et al*., 2019), and this appears to apply to rhizoxins and possibly other *gacA*-regulated antibiotics from *P. protegens* as well. The *gacA*-dependent accumulation of rhizoxins (Hassan *et al*., 2010) may explain the similar patterns observed for the Δ*rzxB* and Δ*gacA* mutants. It needs to be explored if *C. reinhardtii* is able to respond to the harmful effects of *P. protegens*.

In the present study, we have elucidated the complementary and partially overlapping functions of several bacterial secondary metabolites in the interaction between *P. protegens* and *C. reinhardtii*. The extensive morphological changes in *C. reinhardtii* suggest that *P. protegens* functions as an algicidal bacterium. Given the varied roles of *Chlamydomonas* spp. in soil and other habitats, the interactions described herein may have important ecological consequences. While the distribution of the algal-bacterial interaction and the molecular mechanisms described in this work remain to be investigated in different types of soil, *C. reinhardtii* has proven to be a suitable model to characterize the effects of secondary metabolites from soil bacteria on eukaryotic, photosynthetically active organisms in an ecologically meaningful context.

Experimental procedures

Strains and culture conditions

The *C. reinhardtii* strain SAG 73.72 (mt^+) used in this study was obtained from the algal culture collection in Göttingen (Germany). For all Ca^{2+} assays, the aequorin expressing reporter strain AEQ34 based on SAG 73.72 (mt^+) (Aiyar *et al*., 2017) was used. Algal strains were grown in Tris-Acetate-Phosphate (TAP) medium (Harris, 2009). Unless otherwise indicated, the algae were incubated under continuous illumination by fluorescent lamps (Lumilux T8 L36 W/840, Osram Licht AG, Munich, Germany) at 50 μmol photons m^{-2} s^{-1} and agitated on an orbital shaker (200 rpm) at 20°C. *Pseudomonas protegens* Pf-5 (Ramette *et al*., 2011), formerly known as *Pseudomonas fluorescens* Pf-5 (Howell and Stipanovic, 1979), and derived mutants are listed in Table 1. *P. protegens* was likewise grown in TAP medium under continuous illumination except where otherwise stated. Bacterial pre-cultures were agitated in 5 ml medium at 28°C on an orbital shaker (200 rpm) prior to co-culture experiments.

Co-cultivation of C. reinhardtii *and* P. protegens *in liquid culture*

A 3- to 4-day old *C. reinhardtii* pre-culture and an over-night bacterial culture grown in LB medium were washed three times with TAP medium. Algal cell densities were determined by haemocytometer (improved Neubauer chamber, product no. PC73.1, Carl Roth, Karlsruhe, Germany) and bacteria by OD_{600}. Algae and bacteria were inoculated at a starting ratio of 1:100 with a starting concentration of 8.3×10^4 *C. reinhardtii* cells ml^{-1} and 8.3×10^6 *P. protegens* cells ml^{-1}. Using a Multisizer 4e cell counter (Beckman Coulter, Brea CA, USA), the volume of one *C. reinhardtii* cell was estimated to correspond to the volume of ~700 *P. protegens* cells. Cultures were incubated under the algal culture conditions described above.

Co-cultivation and antialgal activity assays on agar plates

For agar tests, 3-day old pre-cultures of *C. reinhardtii* were washed three times with TAP medium. The cell densities were determined with a Multisizer 4e cell counter (Fig. 1, Fig. 3) or with a haemocytometer (Fig. 7) and adjusted to 4×10^6 cells ml^{-1}. Square (120 × 120 mm) or round (Ø 9 mm) Petri dishes were filled half with 2% bacteriological agar (2266.3, Carl Roth) in TAP medium. This bottom layer was overlaid with a top layer of 0.5% bacteriological agar in TAP medium containing the algal cells. For square dishes the top layer contained 4×10^6 cells in 12 ml of top agar, and for round Petri dishes, 2×10^6 cells were used in 5 ml of top agar. Prior to application of *P. protegens* or compounds, round filter disks (Ø 6 mm; KA07.1, Carl Roth) were placed on top of the solidified 0.5% agar layer. Pre-cultures of *P. protegens* were grown in 5 ml LB medium (X968, Carl Roth) for 16 h at 28°C. The cell suspensions were washed three times with TAP medium. Bacterial densities were determined by OD_{600} (Fig. 7) or the Multisizer 4e cell counter (Fig. 1) and then adjusted to a concentration of 7×10^7 cells ml^{-1}. A total volume of 10 μl of this washed and cell-density-adjusted suspension was applied per filter disk. For treatments with standards of individual compounds (see section 'Chemical standards'), 10 μl of methanol containing the amount of substance indicated in Fig. 3C was applied onto a filter disk. The radii of resulting inhibition zones were evaluated after 4 days of incubation under continuous light at 50 μmol photons m^{-2} s^{-1} at a temperature of 20°C.

Antialgal activity assays with compounds in liquid culture

The cell density of a 3-day old *C. reinhardtii* culture was determined with a Multisizer 4e cell counter. Each well of a 24-well plate (CELLSTAR, Greiner, Kremsmünster, Austria) was filled with 1 ml of a cell suspension containing 4×10^6 cells in TAP medium. The individual compounds were dissolved in a volume of 1 or 10 μl of methanol and added to the wells. For treatment with extract, secreted secondary metabolites corresponding to an extract from 3 ml of spent bacterial culture medium were dissolved in methanol and added to 1 ml of algal cell suspension. After incubation for 24 h (50 μmol photons m^{-2} s^{-1} on an orbital shaker at a speed of 200 rpm) the cell densities were determined again with the Multisizer 4e.

Microscopic assessment of algal morphology and flagellation status

Algal cells were fixed with 2.5% (v/v) glutaraldehyde (4157.1, Carl Roth). Brightfield or differential interference

contrast micrographs were recorded using an Axioskop or an Axio Imager M2 microscope (Carl Zeiss, Oberkochen, Germany). ZenBlue software (Carl Zeiss) was used for picture processing.

Motility assay and determination of IC_{50} values

To enrich for motile cells, a 5-day old *C. reinhardtii* 50-ml culture was left to settle for 1 h in darkness. An aliquot of 10 ml cell suspension was taken from the upper region of the liquid culture. The motility assays were performed if at least 75% of the population was motile based on microscopic estimation. Subsequently the cells were counted using a haemocytometer and their density was adjusted to 1×10^6 cells ml^{-1} through the addition of TP medium (TAP medium without acetate adjusted to pH 7.0 with HCl) to avoid further addition of acetate. The cell suspension was then mixed with different concentrations of metabolites (as indicated in Fig. 4A) dissolved in methanol (1% of the total volume). An equal volume of methanol was used as a negative control. After a 5-min incubation period at room temperature and under low light, the number of immotile cells after exposure (n_x) was counted using a haemocytometer. Four squares (volume of one square = 1 mm × 1 mm × 0.1 mm) were counted and averaged per technical replicate. All cells able to stir were considered to be motile. To obtain the total number of cells (n_{tot}), an aliquot of Lugol's iodine solution (5 g iodine and 10 g potassium iodide dissolved in 100 ml H_2O) was added to immobilize all cells. The fraction of motile cells was calculated by subtracting the number of immotile cells from the total cell number as follows: fraction of motile cells = $(n_{tot} - n_x)/n_{tot}$. To determine the half-maximal inhibitory concentration (IC_{50}) values, a curve fitting was carried out in GraphPad PRISM 9 (GraphPad Software, San Diego CA, USA) using a four-parameter non-linear fit based on the equation: $Y = \text{Bottom} + (\text{Top} - \text{Bottom})/(1 + 10\text{^}((\text{Log}(IC_{50}) - X) \text{*HillSlope}))$ where X is the log of the compound concentration, Top is constrained to the mean value of motile cells (in %) of the methanol control treatment, Bottom is constrained to 0% of motile cells, Log(IC_{50}) is the centre of curve, and HillSlope is the slope factor.

Cytosolic Ca^{2+} measurements and Evans blue staining

For Ca^{2+} measurements, the protocol described in Aiyar *et al*. (2017) was followed with the modifications that incubation with coelenterazine was carried out overnight and pre-cultures were grown for 2 days instead of 3 days. Obtained relative luminescence unit (RLU) were converted to molar Ca^{2+} concentrations as described in Fricker *et al*. (1999). For Evans blue staining, the protocol described in (Aiyar *et al*., 2017) was followed. For both assays, algal cultures were grown under 12 h light: 12 h dark cycles at 23°C.

Chemical standards

Standards of orfamide A (sc-391534A), pyoluteorin (sc-391693) and DAPG (sc-206518) were obtained from Santa Cruz Biotechnology (Dallas TX, USA) and pyrrolnitrin (P8861) was obtained from Sigma-Aldrich (St. Louis MO, USA). For the experiments in liquid culture and for the qualitative evaluation of deflagellation, pyoluteorin (≥ 97% HPLC) was purified from *P. protegens* culture extracts (D. Scheer & S. Sasso, unpublished results). Rhizoxin S2 (≥ 95% HPLC) was purified from *Burkholderia rhizoxinica* known to produce rhizoxin S2 using a published method of extraction (Scherlach *et al*., 2006). The identities of purified rhizoxin S2 and pyoluteorin were verified via LC-HRMS (Fig. S8 and Supporting Information, Experimental Procedures) by comparison to an authentic reference.

Extraction of extracellular compounds

To extract secreted secondary metabolites, *P. protegens* was pre-grown in 5 ml TAP medium at 28°C overnight. Thereafter, cells were washed three times with fresh TAP medium and counted with a Multisizer 4e cell counter prior to inoculation of the main culture. A volume of 300 ml TAP medium in 500-ml Erlenmeyer flasks was inoculated with a starting density of 1×10^7 cells ml^{-1} of *P. protegens*. For co-cultures, *C. reinhardtii* was added to the bacterial suspension with an initial cell density of 1×10^5 cells ml^{-1}, resulting in an algal-bacterial starting ratio of 1:100. Cultures were incubated on an orbital shaker at 200 rpm for 48 h until they had reached the stationary phase, with resulting cell densities of 0.95×10^9–2.66×10^9 cells ml^{-1}. To obtain spent medium, the cultures were centrifuged for 20 min at 8000 × *g* at 4°C. The resulting supernatant was extracted twice with an equal volume of HPLC grade ethyl acetate. The solvent was removed by rotation evaporation at 40°C. The dry residue was dissolved in 400 µl of HPLC grade methanol and filtered through a 0.45 µm Ø Chromafil PET filter (729023, Macherey-Nagel, Düren, Germany).

Identification and quantification of secondary metabolites

HPLC was carried out on a Thermo Scientific UltiMate 3000 (Thermo Fisher, Waltham MA, USA). For this, 10 µl of extract were injected and the mixture was separated using a reversed-phase column (Nucleosil 120–5 C18, 250 × 4 mm, CS-Chromatographie Service GmbH, Düren, Germany). The samples were eluted with a binary

gradient consisting of water + 0.1% formic acid (eluent A) and acetonitrile + 0.1% formic acid (eluent B). The gradient started at 98% A and changed linearly to 2% A over a course of 17 min. It was kept at 2% A for another 8 min. The flow rate was maintained constant at 0.8 ml min^{-1}. Eluting substances were detected with a photodiode array (PDA) detector between wavelengths of 200–450 nm.

The analysis of orfamide A was performed by high-resolution mass spectrometry (HRMS) on a QExactive mass spectrometer coupled with an UltiMate 3000 UHPLC using an Accucore column (2.6 μm C18, 100 × 2.1 mm, Thermo Fisher). The orfamide A standard or extracts were eluted with a binary gradient consisting of water + 0.1% formic acid (eluent A) and acetonitrile + 0.1% formic acid (eluent B). The gradient was started at 95% A and changed linearly to 2% A over a course of 10 min and was further kept constant at these conditions for another 4 min. The flow rate was constantly maintained at 0.2 ml min^{-1}. A linear regression using GraphPad PRISM 9 was carried out to obtain standard curves (Fig. S4), and the resulting linear equations were used to calculate metabolite concentrations in extracts.

Acknowledgements

We thank O.C. Chukwuma for preliminary experiments, H. Gross for supplying us with some of the mutants, and E.F.Y. Hom, P. Stallforth, M. Gilbert and D. Carrasco Flores for helpful discussions. M.M.R., D.S., Y.H., A.J.K., P.A. N.M. v.D., C.H., M.M. and S.S. were funded by the Deutsche Forschungsgemeinschaft (DFG, German Research Foundation) – project ID 239748522 – SFB 1127. V.S.H. and P.A. were supported by fellowships of the International Leibniz Research School ILRS (under the head of the Jena School for Microbial Communication). F.V. and N.M.v.D. gratefully acknowledge the support of iDiv funded by the German Research Foundation (DFG–FZT 118, 202548816). Q.Y. and J.E.L. acknowledge funding from the United States Department of Agriculture (USDA), Agricultural Research Service and grant 2011-67019-30192 from the USDA National Institute of Food and Agriculture.

Conflict of interest

The authors declare no conflict of interest.

References

Aiyar, P., Schaeme, D., García-Altares, M., Carrasco Flores, D., Dathe, H., Hertweck, C., *et al*. (2017) Antagonistic bacteria disrupt calcium homeostasis and immobilize algal cells. *Nat Commun* **8**: 1756.

Alvarez, A.L., Weyers, S.L., Goemann, H.M., Peyton, B.M., and Gardner, R.D. (2021) Microalgae, soil and plants: a critical review of microalgae as renewable resources for agriculture. *Algal Res* **54**: 102200.

Behrenfeld, M.J., Randerson, J.T., McClain, C.R., Feldman, G.C., Los, S.O., Tucker, C.J., *et al*. (2001) Biospheric primary production during an ENSO transition. *Science* **291**: 2594–2597.

Brazelton, J.N., Pfeufer, E.E., Sweat, T.A., McSpadden Gardener, B.B., and Coenen, C. (2008) 2,4-diacetylphloroglucinol alters plant root development. *Mol Plant Microbe Interact* **21**: 1349–1358.

Brendel, N., Partida-Martinez, L.P., Scherlach, K., and Hertweck, C. (2007) A cryptic PKS-NRPS gene locus in the plant commensal *Pseudomonas fluorescens* Pf-5 codes for the biosynthesis of an antimitotic rhizoxin complex. *Org Biomol Chem* **5**: 2211–2213.

Crutchfield, A.L.M., Diller, K.R., and Brand, J.J. (1999) Cryopreservation of *Chlamydomonas reinhardtii* (Chlorophyta). *Eur J Phycol* **34**: 43–52.

Ding, T., Yang, L.-J., Zhang, W.-D., and Shen, Y.-H. (2020) Pyoluteorin induces cell cycle arrest and apoptosis in human triple-negative breast cancer cells MDA-MB-231. *J Pharm Pharmacol* **72**: 969–978.

Elbert, W., Weber, B., Burrows, S., Steinkamp, J., Büdel, B., Andreae, M.O., and Pöschl, U. (2012) Contribution of cryptogamic covers to the global cycles of carbon and nitrogen. *Nat Geosci* **5**: 459–462.

Fricker, M.D., Plieth, C., Knight, H., Blancaflor, E., Knight, M. R., White, N.S., and Gilroy, S. (1999) Fluorescence and luminescence techniques to probe ion activities in living plant cells. In *Fluorescent and Luminescent Probes for Biological Activity*, 2nd ed, Mason, W.T. (ed). San Diego: Academic Press, pp. 569–596.

Gross, H., and Loper, J.E. (2009) Genomics of secondary metabolite production by *Pseudomonas* spp. *Nat Prod Rep* **26**: 1408–1446.

Gross, H., Stockwell, V.O., Henkels, M.D., Nowak-Thompson, B., Loper, J.E., and Gerwick, W.H. (2007) The genomisotopic approach: a systematic method to isolate products of orphan biosynthetic gene clusters. *Chem Biol* **14**: 53–63.

Haas, D., and Défago, G. (2005) Biological control of soil-borne pathogens by fluorescent pseudomonads. *Nat Rev Microbiol* **3**: 307–319.

Harris, E.H. (2009) *Chlamydomonas* in the laboratory. In *The Chlamydomonas Sourcebook*, 2nd ed, Harris, E.H., Stern, D.B., and Witman, G.B. (eds). Oxford: Academic Press, pp. 241–302.

Hartney, S.L., Mazurier, S., Kidarsa, T.A., Quecine, M.C., Lemanceau, P., and Loper, J.E. (2011) TonB-dependent outer-membrane proteins and siderophore utilization in *Pseudomonas fluorescens* Pf-5. *Biometals* **24**: 193–213.

Hassan, K.A., Johnson, A., Shaffer, B.T., Ren, Q., Kidarsa, T.A., Elbourne, L.D.H., *et al*. (2010) Inactivation of the GacA response regulator in *Pseudomonas fluorescens* Pf-5 has far-reaching transcriptomic consequences. *Environ Microbiol* **12**: 899–915.

Henkels, M.D., Kidarsa, T.A., Shaffer, B.T., Goebel, N.C., Burlinson, P., Mavrodi, D.V., *et al*. (2014) *Pseudomonas protegens* Pf-5 causes discoloration and pitting of mushroom caps due to the production of antifungal metabolites. *Mol Plant Microbe Interact* **27**: 733–746.

Hochmal, A.K., Zinzius, K., Charoenwattanasatien, R., Gäbelein, P., Mutoh, R., Tanaka, H., *et al*. (2016) Calredoxin represents a novel type of calcium-dependent sensor-responder connected to redox regulation in the chloroplast. *Nat Commun* **7**: 11847.

Hom, E.F.Y., Aiyar, P., Schaeme, D., Mittag, M., and Sasso, S. (2015) A chemical perspective on microalgal-microbial interactions. *Trends Plant Sci* **20**: 689–693.

Howell, C.R., and Stipanovic, R.D. (1979) Control of *Rhizoctonia solani* on cotton seedlings with *Pseudomonas fluorescens* and with an antibiotic produced by the bacterium. *Phytopathology* **69**: 480–482.

Howell, C.R., and Stipanovic, R.D. (1980) Suppression of *Pythium ultimum*-induced damping-off of cotton seedlings by *Pseudomonas fluorescens* and its antibiotic, pyoluteorin. *Phytopathology* **70**: 712–715.

Kidarsa, T.A., Goebel, N.C., Zabriskie, T.M., and Loper, J.E. (2011) Phloroglucinol mediates cross-talk between the pyoluteorin and 2,4-diacetylphloroglucinol biosynthetic pathways in *Pseudomonas fluorescens* Pf-5. *Mol Microbiol* **81**: 395–414.

Kidarsa, T.A., Shaffer, B.T., Goebel, N.C., Roberts, D.P., Buyer, J.S., Johnson, A., *et al*. (2013) Genes expressed by the biological control bacterium *Pseudomonas protegens* Pf-5 on seed surfaces under the control of the global regulators GacA and RpoS. *Environ Microbiol* **15**: 716–735.

Kwak, Y.-S., Han, S., Thomashow, L.S., Rice, J.T., Paulitz, T.C., Kim, D., and Weller, D.M. (2011) *Saccharomyces cerevisiae* genome-wide mutant screen for sensitivity to 2,4-diacetylphloroglucinol, an antibiotic produced by *Pseudomonas fluorescens*. *Appl Environ Microbiol* **77**: 1770–1776.

Loper, J.E., Henkels, M.D., Shaffer, B.T., Valeriote, F.A., and Gross, H. (2008) Isolation and identification of rhizoxin analogs from *Pseudomonas fluorescens* Pf-5 by using a genomic mining strategy. *Appl Environ Microbiol* **74**: 3085–3093.

Loper, J.E., Henkels, M.D., Rangel, L.I., Olcott, M.H., Walker, F.L., Bond, K.L., *et al*. (2016) Rhizoxin analogs, orfamide A and chitinase production contribute to the toxicity of *Pseudomonas protegens* strain Pf-5 to *Drosophila melanogaster*. *Environ Microbiol* **18**: 3509–3521.

Loper, J.E., Hassan, K.A., Mavrodi, D.V., Davis, E.W., II, Lim, C.K., Shaffer, B.T., *et al*. (2012) Comparative genomics of plant-associated *Pseudomonas* spp.: insights into diversity and inheritance of traits involved in multitrophic interactions. *PLoS Genet* **8**: e1002784.

Mayali, X., and Azam, F. (2004) Algicidal bacteria in the sea and their impact on algal blooms. *J Eukaryotic Microbiol* **51**: 139–144.

Metting, B. (1986) Population dynamics of *Chlamydomonas sajao* and its influence on soil aggregate stabilization in the field. *Appl Environ Microbiol* **51**: 1161–1164.

Meyer, N., Bigalke, A., Kaulfuß, A., and Pohnert, G. (2017) Strategies and ecological roles of algicidal bacteria. *FEMS Microbiol Rev* **41**: 880–899.

Nestler, H., Groh, K.J., Schönenberger, R., Behra, R., Schirmer, K., Eggen, R.I., and Suter, M.J.-F. (2012) Multiple-endpoint assay provides a detailed mechanistic view of responses to herbicide exposure in *Chlamydomonas reinhardtii*. *Aquat Toxicol* **110-111**: 214–224.

Nowak-Thompson, B., Gould, S.J., Kraus, J., and Loper, J. E. (1994) Production of 2,4-diacetylphloroglucinol by the biocontrol agent *Pseudomonas fluorescens* Pf-5. *Can J Microbiol* **40**: 1064–1066.

Paulsen, I.T., Press, C.M., Ravel, J., Kobayashi, D.Y., Myers, G.S.A., Mavrodi, D.V., *et al*. (2005) Complete genome sequence of the plant commensal *Pseudomonas fluorescens* Pf-5. *Nat Biotechnol* **23**: 873–878.

Prota, A.E., Bargsten, K., Diaz, J.F., Marsh, M., Cuevas, C., Liniger, M., *et al*. (2014) A new tubulin-binding site and pharmacophore for microtubule-destabilizing anticancer drugs. *Proc Natl Acad Sci U S A* **111**: 13817–13821.

Quecine, M.C., Kidarsa, T.A., Goebel, N.C., Shaffer, B.T., Henkels, M.D., Zabriskie, T.M., and Loper, J.E. (2016) An interspecies signaling system mediated by fusaric acid has parallel effects on antifungal metabolite production by *Pseudomonas protegens* strain Pf-5 and antibiosis of *Fusarium* spp. *Appl Environ Microbiol* **82**: 1372–1382.

Ramanan, R., Kim, B.-H., Cho, D.-H., Oh, H.-M., and Kim, H.-S. (2016) Algae-bacteria interactions: evolution, ecology and emerging applications. *Biotechnol Adv* **34**: 14–29.

Ramette, A., Frapolli, M., Fischer-Le Saux, M., Gruffaz, C., Meyer, J.-M., Défago, G., *et al*. (2011) *Pseudomonas protegens* sp. nov., widespread plant-protecting bacteria producing the biocontrol compounds 2,4-diacetylphloroglucinol and pyoluteorin. *Syst Appl Microbiol* **34**: 180–188.

Rosenbaum, J.L., Moulder, J.E., and Ringo, D.L. (1969) Flagellar elongation and shortening in *Chlamydomonas*. The use of cycloheximide and colchicine to study the synthesis and assembly of flagellar proteins. *J Cell Biol* **41**: 600–619.

Sasso, S., Stibor, H., Mittag, M., and Grossman, A.R. (2018) From molecular manipulation of domesticated *Chlamydomonas reinhardtii* to survival in nature. *Elife* **7**: e39233.

Scherlach, K., Partida-Martinez, L.P., Dahse, H.M., and Hertweck, C. (2006) Antimitotic rhizoxin derivatives from a cultured bacterial endosymbiont of the rice pathogenic fungus *Rhizopus microsporus*. *J Am Chem Soc* **128**: 11529–11536.

Schmidt, O., Dyckmans, J., and Schrader, S. (2016) Photoautotrophic microorganisms as a carbon source for temperate soil invertebrates. *Biol Lett* **12**: 20150646.

Schmidt, R., Ulanova, D., Wick, L.Y., Bode, H.B., and Garbeva, P. (2019) Microbe-driven chemical ecology: past, present and future. *ISME J* **13**: 2656–2663.

Takahashi, M., Matsumoto, S., Iwasaki, S., and Yahara, I. (1990) Molecular basis for determining the sensitivity of eucaryotes to the antimitotic drug rhizoxin. *Mol Gen Genet* **222**: 169–175.

Tripathi, R.K., and Gottlieb, D. (1969) Mechanism of action of antifungal antibiotic pyrrolnitrin. *J Bacteriol* **100**: 310–318.

Troppens, D.M., Dmitriev, R.I., Papkovsky, D.B., O'Gara, F., and Morrissey, J.P. (2013a) Genome-wide investigation of cellular targets and mode of action of the antifungal bacterial metabolite 2,4-diacetylphloroglucinol in *Saccharomyces cerevisiae*. *FEMS Yeast Res* **13**: 322–334.

Troppens, D.M., Chu, M., Holcombe, L.J., Gleeson, O., O'Gara, F., Read, N.D., and Morrissey, J.P. (2013b) The bacterial secondary metabolite 2,4-diacetylphloroglucinol impairs mitochondrial function and affects calcium homeostasis in *Neurospora crassa*. *Fungal Genet Biol* **56**: 135–146.

Weller, D.M., Raaijmakers, J.M., McSpadden Gardener, B. B., and Thomashow, L.S. (2002) Microbial populations responsible for specific soil suppressiveness to plant pathogens. *Annu Rev Phytopathol* **40**: 309–348.

Westhoff, S., Otto, S.B., Swinkels, A., Bode, B., van Wezel, G.P., and Rozen, D.E. (2019) Spatial structure increases the benefits of antibiotic production in *Streptomyces*. *Evolution* **74**: 179–187.

Wheeler, G.L., Joint, I., and Brownlee, C. (2008) Rapid spatiotemporal patterning of cytosolic Ca^{2+} underlies flagellar excision in *Chlamydomonas reinhardtii*. *Plant J* **53**: 401–413.

Wiener, P. (2001) Antibiotic production in a spatially structured environment. *Ecol Lett* **3**: 122–130.

Yan, Q., Lopes, L.D., Shaffer, B.T., Kidarsa, T.A., Vining, O., Philmus, B., *et al*. (2018) Secondary metabolism and interspecific competition affect accumulation of spontaneous mutants in the GacS-GacA regulatory system in *Pseudomonas protegens*. *mBio*: **9**: e01845-17.

Yordanova, Z.P., Woltering, E.J., Kapchina-Toteva, V.M., and Iakimova, E.T. (2013) Mastoparan-induced programmed cell death in the unicellular alga *Chlamydomonas reinhardtii*. *Ann Bot* **111**: 191–205.

Youngblom, J., Schloss, J.A., and Silflow, C.D. (1984) The two β-tubulin genes of *Chlamydomonas reinhardtii* code for identical proteins. *Mol Cell Biol* **4**: 2686–2696.

Supporting Information

Additional Supporting Information may be found in the online version of this article at the publisher's web-site:

Appendix S1. Supporting Information.

Table S1. Summary of growth inhibition of *Pseudomonas protegens* (wild type and mutants) on *Chlamydomonas reinhardtii* in agar plate assays.

Fig. S1. Individual secondary metabolites severely alter the morphology of *Chlamydomonas reinhardtii* cells after prolonged exposure. Five representative micrographs of *C. reinhardtii* cells after 24 h of cultivation with or without orfamide A, pyoluteorin, DAPG, pyrrolnitrin, rhizoxin S2 or the total extracted secondary metabolites are shown. Note that a small fraction of cells were morphologically unaltered in all treatments except for cells treated with pyrrolnitrin. 0.1% methanol served as the negative control for orfamide A and pyrrolnitrin while 1% methanol was the negative control for all other treatments. This experiment was performed twice in three biological replicates. For each replicate a minimum of 10 cells were photographed.

Fig. S2. Additional Ca^{2+} curves (those not shown in Fig. 1C and Fig. 5A). **A** Effects of the mixture and of individual compounds extracted from *Pseudomonas protegens* culture supernatants on cytosolic Ca^{2+} levels in *Chlamydomonas reinhardtii*. A black arrowhead indicates the addition of extract. As a negative control, methanol equivalent to the volume of extract dissolved in methanol was used. **B** Effects of DAPG, pyrrolnitrin and pyoluteorin on cytosolic Ca^{2+} levels in *C. reinhardtii*. Black arrowheads indicate the addition of treatments. As negative controls ethanol was used for pyoluteorin and methanol for DAPG and pyrrolnitrin. In both panels, each line in the diagrams represents the mean of three biological replicates, and each biological replicate includes three technical replicates.

Fig. S3. Pyoluteorin, DAPG, pyrrolnitrin, rhizoxin S2 and orfamide A are present in culture supernatants of Pseudomonas protegens grown in TAP medium. **A** Chromatograms from extracted secondary metabolites isolated from spent medium of 2-day-old axenically grown *P. protegens* cultures, cultivated in TAP medium (black lines). Each chromatogram was further overlaid with a respective chromatogram from the same extract spiked with pyoluteorin, 2,4-diacetylphloroglucinol (DAPG), pyrrolnitrin or rhizoxin S2 standards (colored lines). **B** Detection of orfamide A in extracts by LC-HRMS. Calculated prediction for the positive ion of C64H115O17N10 as $[M+H]+$: $m/z = 1295.8436$.

Fig. S4. Standard curves for the quantification of extracted secondary metabolites. **A** Standard curves for pyoluteorin, pyrrolnitrin, DAPG and rhizoxin S2 (HPLC). Five different concentrations were measured in 3 technical replicates, and peak areas were integrated at their λ_{max} absorption wavelengths. **B** Standard curve for orfamide A generated by LC-HRMS. Six different concentrations were measured in 3 technical replicates, and the areas of the ion intensity peaks were integrated. In all panels, the equations resulting from linear regression are indicated. The resulting equations were used to calculate the concentrations of pyoluteorin, DAPG, pyrrolnitrin, rhizoxin S2 and orfamide A in the previously obtained chromatograms for P. protegens extracts.

Fig. S5. Rhizoxin S2 does not immobilize or deflagellate Chlamydomonas reinhardtii at a concentration of 160 μM. **A** Trial for the determination of a half-maximal inhibitory concentration (IC50) for algal motility after treatment with rhizoxin S2. The mean ± SD are shown and empty squares indicate the methanol control. No significant inhibitory effect on algal motility was detected after 5 min of treatment with a concentration of 160 μM rhizoxin S2. This experiment was carried three times independently in three technical replicates each. For the statistical analysis, a student's t-test was performed. No statistically significant difference was found (ns = not significant). **B** Representative micrographs of C. reinhardtii treated with rhizoxin S2 for 1 or 5 min. Methanol was applied as a negative control. The presence of flagella is highlighted with black arrowheads.

Fig. S6. Photographs of additional liquid co-cultures of *Chlamydomonas reinhardtii* and *Pseudomonas protegens* mutants (those not shown in Fig. 7B). For more information on the mutants see Table 1.

Fig. S7. Additional micrographs showing how algal morphology is affected by different *Pseudomonas protegens mutants* (those not shown in Fig. 7C). For more information on the mutants see Table 1.

Fig. S8. Mass spectra of purified pyoluteorin and rhizoxin S2 A m/z value corresponding to the nominal mass of rhizoxin S2. The fully recorded range is depicted (m/z

115-1500). Calculated prediction for the positive ion of C35H50O9N as [M+H]+: m/z = 628.3480 B m/z value corresponding to the nominal mass of pyoluteorin. A full range was recorded at m/z 50-1500. Calculated prediction for the positive ion of C11H8O3NCl2 as [M+H]+: m/z = 271.9876. The original chromatogram and mass spectrum as well as spectral interpretations are available on the MassBank of North America and the iDiv data repository: (https://mona.fiehnlab.ucdavis.edu/spectra/display/MoNA023820) https://idata.idiv.de/ project ID: 3465.